

**Symmetry breaking in a  
bulk-surface reaction-diffusion  
model for signaling networks**

Andreas Rätz and Matthias Röger

Preprint 2013-07

Mai 2013



# SYMMETRY BREAKING IN A BULK–SURFACE REACTION–DIFFUSION MODEL FOR SIGNALING NETWORKS

ANDREAS RÄTZ AND MATTHIAS RÖGER

ABSTRACT. Signaling molecules play an important role for many cellular functions. We investigate here a general system of two membrane reaction–diffusion equations coupled to a diffusion equation inside the cell by a Robin-type boundary condition and a flux term in the membrane equations. A specific model of this form was recently proposed by the authors for the GTPase cycle in cells. We investigate here a putative role of diffusive instabilities in cell polarization. By a linearized stability analysis we identify two different mechanisms. The first resembles a classical Turing instability for the membrane subsystem and requires (unrealistically) large differences in the lateral diffusion of activator and substrate. The second possibility on the other hand is induced by the difference in cytosolic and lateral diffusion and appears much more realistic. We complement our theoretical analysis by numerical simulations that confirm the new stability mechanism and allow to investigate the evolution beyond the regime where the linearization applies.

## 1. INTRODUCTION

In numerous biological processes the emergence and maintenance of polarized states in the form of heterogeneous distributions of chemical substances (proteins, lipids) is essential. Such symmetry breaking for example precedes the formation of buds in yeast cells, determines directions of movement, or mediates differentiation and development of cells. Polarized states in biological cells often arise in response to external signals, typically from the outer cell membrane. Transport processes and interacting networks of diffusing and reacting substances both within the cell and on the cell membrane then amplify and process such signals. The distribution of small GTPase molecules in eukaryotic cells presents one example of a complex system with polarization and motivates the present paper. Such molecules can be in an active and in an inactive state. Activation and deactivation typically occurs at the cell membrane and is catalyzed by specific enzymes. In addition to the activation–deactivation cycle GTPase molecules (in its inactive form) shuttle between the membrane and the cytosol, i.e. the inner volume of the cell, by attachment to and detachment from the membrane. These properties induce the specific form of a coupled volume (bulk) and surface reaction–diffusion system. The goal here is to investigate a possible contribution of diffusive instabilities to cell polarization in such coupled systems.

Different deterministic continuous models have been used to investigate polarization of cells (see for example the review [8]). We consider here a particular class of models that takes the form of a reaction-diffusion system on the membrane coupled to a diffusion process in the interior of the cell. This model has been introduced in [17] where a reduction to a non-local reaction-diffusion system, involving only membrane variables, has been investigated. A key question in such systems is whether a Turing-type mechanism may contribute to the polarization of cells, with activated GTPase and inactive GTPase representing self-activator and substrate, respectively. Turing-type instabilities however require large differences in the diffusion constants for activator and substrate (or inhibitor). The lateral diffusion on the membrane for active and inactive GTPase on the other hand is in general of comparable size and therefore a Turing instability appears at

---

*Date:* May 27, 2013.

*2000 Mathematics Subject Classification.* 92C37,35K57,35Q92.

*Key words and phrases.* Reaction-diffusion systems, PDEs on surfaces, Turing instability, numerical simulations of reaction-diffusion systems.

first glance unrealistic. On the other hand, cytosolic diffusion in cells is typically much faster than lateral diffusion and might induce the necessary difference in diffusion. It is therefore tempting to hypothesize that in such coupled 2D and 3D reaction–diffusion systems diffusive instabilities can in fact contribute to cell polarization.

We will in the following represent the cytosolic volume and the membrane of a cell by a bounded, connected, open domain  $B \subset \mathbb{R}^3$  in space and its two-dimensional boundary  $\Gamma := \partial B$  respectively. We assume that  $\Gamma$  is given by a smooth, closed surface and denote by  $\nu$  the outer unit normal of  $B$  on  $\Gamma$ . Further we fix a time interval of observation  $I := [0, T] \subset \mathbb{R}$  and consider smooth functions  $V : \bar{B} \times I \rightarrow \mathbb{R}$ ,  $u, v : \Gamma \times I \rightarrow \mathbb{R}$  (representing the cytosolic inactive, membrane-bound active, and membrane-bound inactive GTPase, respectively) that satisfy the coupled reaction–diffusion system (stated in a non-dimensional form)

$$\partial_t V = D\Delta V \quad \text{in } B \times I, \quad (1.1)$$

$$\partial_t u = \Delta_\Gamma u + \gamma f(u, v) \quad \text{on } \Gamma \times I, \quad (1.2)$$

$$\partial_t v = d\Delta_\Gamma v + \gamma(-f(u, v) + q(u, v, V)) \quad \text{on } \Gamma \times I, \quad (1.3)$$

$$-D\nabla V \cdot \nu = \gamma q(u, v, V) \quad \text{on } \Gamma \times I. \quad (1.4)$$

Here  $f$  and  $g$  represent the activation/inactivation processes and  $q$  describes attachment/detachment at the membrane. In the appendix we present as specific example the mathematical model for the GTPase cycle from [17] with explicit choices for  $f$  and  $q$  that we also use in our numerical simulations below. The parameter  $\gamma > 0$  is a non-dimensional parameter that is related to the spatial scale of the cell. The coupling of bulk and surface processes in (1.1)–(1.4) is given in form of a Robin-type boundary condition. The system is complemented by initial conditions at time  $t = 0$ ,

$$\begin{aligned} V(\cdot, 0) &= V_0, & v(\cdot, 0) &= v_0, & u(\cdot, 0) &= u_0, \\ V_0 : B &\rightarrow \mathbb{R}, & v_0, u_0 &: \Gamma \rightarrow \mathbb{R}. \end{aligned}$$

We remark that the system (1.1)–(1.4) automatically satisfies conservation of total mass, i.e.

$$M(t) := \int_B V(x, t) \, dx + \int_\Gamma (u + v)(x, t) \, d\sigma(x) = \text{const},$$

where  $d\sigma$  denotes integration with respect to the surface area measure.

In this contribution we investigate the possibility of diffusive instabilities for systems of the form (1.1)–(1.4). We present a linear stability analysis and numerical simulations. We find two possible scenarios for a diffusive instability of spatially homogeneous stationary states. The first needs large differences in lateral diffusion for  $u$  and  $v$  (i.e. a coefficient  $d \gg 1$ ) and resembles a classical Turing instability in the  $u, v$  variables. The second mechanism on the other hand does also occur for equal lateral diffusion constants  $d = 1$  and is rather based on the different diffusion constants for  $u$  and  $V$  and therefore on the coupling of bulk and surface equations. As cytosolic diffusion is typically by a factor hundred faster than lateral diffusion, this scenario is much more realistic in the application to signaling networks. In Section 3 we compare the stability of the full system to its reduction in the formal limit  $D \rightarrow \infty$ . The latter leads to a non-local two-variable system on the membrane that has been analyzed in [17] (see also [19]). There we have only covered the first more ‘classical’ instability mechanism and have not included a complete characterization of diffusive instabilities. Here we show that – in coincidence with the case  $D < \infty$  – we again have the same alternative scenarios for diffusive instabilities. Some specific properties of the second instability mechanism are easier to characterize in the reduction. In particular we find that the second scenario is different from a standard Turing-type instability as in this case the concentration of activated GTPase in a single spot (most typical in most examples of cell polarization) is always preferred independent of variations in the parameter values. This robustness makes the second instability mechanism an even more attractive explanation for polarization. In Section 4 we present numerical simulations for specific versions both of the full system (1.1)–(1.4) and of the

reduced system. The simulations confirm the instability criteria derived for the linearised system and allow to investigate the time-evolution after the onset of heterogeneities and beyond the regime governed by the linearization. It turns out that even for simple choices of the constitutive relations  $f$  and  $q$  the system exhibits a rich behavior. In the final Section 6 we discuss the results of the paper and in particular comment on the term ‘diffuse instability’ in the present context and with respect to the second instability mechanism.

The most specific property of the model considered here is the coupling of bulk and surface reaction–diffusion systems. Such coupled systems often arise in cell biology where enzymatic processes on intracellular membranes play a role, see [15] and the references therein. Surface–bulk reaction–diffusion or convection–diffusion systems also arise in the modeling of surfactants on two-fluid interfaces [20]. Coupled surface–bulk systems have been studied intensively over the last decades by numerical simulations, see for example [13, 20, 6, 15, 3] and the references therein.

In [13] a model that is similar to ours and that describes a two-variable diffusion system in a volume coupled to a reaction system on the boundary has been studied. Here the authors provide numerical simulations and a linear stability analysis. They show the existence of Turing instabilities in their model, even for equal bulk diffusion constants. The main difference to our model is that in [13] both activator and substrate diffuse in the bulk and that no diffusion on the membrane surface is considered.

## 2. STABILITY ANALYSIS FOR THE FULL SYSTEM

We consider in the following the spatially coupled reaction–diffusion system (1.1)–(1.4) for spherical cell shapes and investigate the possibility of diffusive instabilities of a homogeneous stationary state. Because of the different domains of definition of  $V$  and  $u, v$  we cannot apply standard conditions for (in)stability and therefore will derive appropriate criteria in this section. Similar to a classical Turing instability we consider a spatially homogeneous stationary state and require that this state is (a) stable against perturbations of the membrane quantities  $u, v$  that are spatially homogeneous *on the membrane* and perturbations of the bulk variable  $V$  that are radially symmetric (this additional restriction follows already by the first) and (b) unstable with respect to general perturbations. Such property represents a diffusive instability and a symmetry breaking in the sense that the radially symmetric evolution loses its stability as it approaches such a stationary point.

For the constitutive relations  $f, q$  we assume that

$$\partial_v f \geq 0, \quad \partial_v q \leq 0, \quad \partial_v q \leq \partial_u q, \quad \partial_V q \geq 0, \quad (2.1)$$

which are for the application to the GTPase cycle natural conditions with respect to the interpretation of  $f$  as activation rate and  $q$  as the flux induced by ad- and desorption of GTPase at the membrane. As we are interested in symmetry breaking we consider in the following a spatially homogeneous stationary state  $(u_*, v_*, V_*) \in \mathbb{R}_+^3 := \{(x_1, x_2, x_3) \in \mathbb{R}^3 : x_i > 0, i = 1, 2, 3\}$  of (1.1)–(1.4), which is equivalent to the conditions

$$f(u_*, v_*) = 0, \quad (2.2)$$

$$q(u_*, v_*, V_*) = 0. \quad (2.3)$$

For convenience we introduce the following notation,

$$\begin{aligned} f_u &:= \partial_u f(u_*, v_*), & f_v &:= \partial_v f(u_*, v_*), \\ q_u &:= \partial_u q(u_*, v_*, V_*), & q_v &:= \partial_v q(u_*, v_*, V_*), & q_V &:= \partial_V q(u_*, v_*, V_*). \end{aligned} \quad (2.4)$$

We assume that in  $(V_*, u_*, v_*)$  we have strict inequalities

$$f_v > 0, \quad q_v < 0, \quad q_V > 0, \quad (2.5)$$

The linearization of (1.1)–(1.4) in  $(V_*, u_*, v_*)$  is given by the system

$$\partial_t V = D\Delta V \quad \text{in } B \times I, \quad (2.6)$$

$$\partial_t u = \Delta_\Gamma u + \gamma(f_u u + f_v v) \quad \text{on } \Gamma \times I, \quad (2.7)$$

$$\partial_t v = d\Delta_\Gamma v + \gamma((-f_u + q_u)u + (-f_v + q_v)v + q_V V) \quad \text{on } \Gamma \times I, \quad (2.8)$$

$$-D\nabla V \cdot \nu = \gamma(q_u u + q_v v + q_V V) \quad \text{on } \Gamma \times I \quad (2.9)$$

for unknowns  $V : B \times \mathbb{R} \rightarrow \mathbb{R}$ ,  $u, v : \Gamma \times \mathbb{R} \rightarrow \mathbb{R}$ , together with a constraint on the initial conditions, due to the mass conservation property,

$$\int_B V(x, 0) dx + \int_\Gamma (u(x, 0) + v(x, 0)) d\sigma(x) = 0. \quad (2.10)$$

In the following we assume that no inner membranes are present and assume a spherical shape of the cell, i.e. we choose  $B = B_1(0)$  and  $\Gamma = \partial B = S^2$ . This allows in the subsequent stability analysis to use separated variables: we introduce polar coordinates and represent  $x \in B$  as  $x = ry$  with  $y \in S^2$ ,  $r \in [0, 1]$ . We further fix an orthonormal basis  $\{\varphi_{lm}\}_{l \in \mathbb{N}_0, m \in \mathbb{Z}, |m| \leq l}$  of  $L^2(\Gamma)$  given by spherical harmonics with

$$-\Delta_\Gamma \varphi_{lm} = l(l+1)\varphi_{lm} \quad \text{on } \Gamma \quad (2.11)$$

and remark that  $\varphi_{00}$  is constant on  $\Gamma$ . We then consider the following ansatz for solution of the linearized system (2.6)–(2.9),

$$u(y, t) = \sum_{l \in \mathbb{N}_0, m \in \mathbb{Z}, |m| \leq l} u_{lm}(t) \varphi_{lm}(y), \quad (2.12)$$

$$v(y, t) = \sum_{l \in \mathbb{N}_0, m \in \mathbb{Z}, |m| \leq l} v_{lm}(t) \varphi_{lm}(y), \quad (2.13)$$

$$V(ry, t) = \sum_{l \in \mathbb{N}_0, m \in \mathbb{Z}, |m| \leq l} V_{lm}(t) \psi_{lm}(r) \varphi_{lm}(y), \quad (2.14)$$

with  $u_{lm}, v_{lm}, V_{lm} : \mathbb{R} \rightarrow \mathbb{R}$ ,  $\psi_{lm} : [0, 1] \rightarrow \mathbb{R}$ ,  $y \in \Gamma$ ,  $0 \leq r \leq 1$  (for a similar approach see [13]). We deduce from (2.6)–(2.9), by taking the  $L^2(\Gamma)$  scalar product with  $\varphi_{lm}$ ,

$$u'_{lm} = -l(l+1)u_{lm} + \gamma(f_u u_{lm} + f_v v_{lm}), \quad (2.15)$$

$$v'_{lm} = -dl(l+1)v_{lm} + \gamma((-f_u + q_u)u_{lm} + (-f_v + q_v)v_{lm} + q_V \psi_{lm}(1)V_{lm}), \quad (2.16)$$

$$V'_{lm}(t) \psi_{lm}(r) = DV_{lm}(t) \left( \psi''_{lm}(r) + \frac{2}{r} \psi'_{lm}(r) - \frac{1}{r^2} l(l+1) \psi_{lm}(r) \right), \quad (2.17)$$

$$-DV_{lm} \psi'_{lm}(1) = \gamma(q_u u_{lm} + q_v v_{lm} + q_V \psi_{lm}(1)V_{lm}). \quad (2.18)$$

From (2.17) we obtain that

$$V_{lm}(t) = \bar{B}_{lm} e^{\omega_{lm} t}, \quad \bar{B}_{lm} \in \mathbb{R}, \quad \omega_{lm} \in \mathbb{R}, \quad (2.19)$$

and  $V_{lm}$  is either identically zero or does nowhere vanish.

In the following we first restrict ourselves to the case  $V_{lm} \neq 0$ . We deduce that

$$0 = r^2 \psi''_{lm}(r) + 2r \psi'_{lm}(r) - \left( l(l+1) + \frac{\omega_{lm}}{D} r^2 \right) \psi_{lm}(r). \quad (2.20)$$

If in addition  $\omega_{lm} > 0$ , the latter equation implies that

$$\psi_{lm}(r) = \alpha_{lm} i_l \left( \sqrt{\frac{\omega_{lm}}{D}} r \right), \quad \alpha_{lm} \in \mathbb{R}, \quad (2.21)$$

$$i_l(r) = \sqrt{\frac{\pi}{2r}} I_{l+\frac{1}{2}}(r),$$

where  $I_{l+\frac{1}{2}}$  denotes the respective modified Bessel functions of first kind. In the case  $\omega_{lm} = 0$  we obtain instead

$$\psi_{lm}(r) = \alpha_{lm} r^l, \alpha_{lm} \in \mathbb{R}. \quad (2.22)$$

We derive from (2.15), (2.16), (2.19) and (2.18) the linear ODE system

$$u'_{lm} = (-l(l+1) + \gamma f_u)u_{lm} + \gamma f_v v_{lm}, \quad (2.23)$$

$$v'_{lm} = -\gamma f_u u_{lm} - (dl(l+1) + \gamma f_v)v_{lm} - D\psi'_{lm}(1)V_{lm}, \quad (2.24)$$

$$V'_{lm} = \omega_{lm} V_{lm}, \quad (2.25)$$

coupled to an algebraic equation

$$0 = \gamma(q_u u_{lm} + q_v v_{lm}) + (\gamma q_V \psi_{lm}(1) + D\psi'_{lm}(1))V_{lm}, \quad (2.26)$$

that determines in the case  $V_{lm} \neq 0$  together with (2.21) the value of  $\omega_{lm}$ . The linear stability analysis then reduces to an analysis of the eigenvalue equation coupled to an algebraic condition. We obtain that an eigenvalue  $\omega$  with nonnegative real part exists if and only if first  $\omega = \omega_{lm} \in \mathbb{R}_0^+$  and second  $\omega_{lm}$  satisfies

$$\begin{aligned} 0 &\stackrel{!}{=} G_l(\omega_{lm}) \\ &:= \gamma q_V \left( \omega_{lm}^2 + ((d+1)l(l+1) + (-f_u + f_v)\gamma)\omega_{lm} + dl^2(l+1)^2 + \gamma l(l+1)(-df_u + f_v) \right) \\ &\quad + \kappa_{D,l}(\omega_{lm}) \left( \omega_{lm}^2 + ((d+1)l(l+1) + (-f_u + f_v)\gamma)\omega_{lm} + \right. \\ &\quad \quad \left. + dl^2(l+1)^2 + \gamma l(l+1)(-df_u + f_v) \right) \\ &\quad + \kappa_{D,l}(\omega_{lm}) \left( -\gamma q_v(l(l+1) + \omega_{lm}) + \gamma^2(f_u q_v - f_v q_u) \right) \end{aligned} \quad (2.27)$$

with

$$\kappa_{D,l}(\omega) := \frac{D\psi'_{lm}(1)}{\psi_{lm}(1)} = D \left( \frac{r i'_l(r)}{i_l(r)} \right) \Big|_{r=\sqrt{\frac{\omega}{D}}}, \quad (2.28)$$

where the last equality follows for  $\omega > 0$  from (2.21) and for  $\omega_{lm} = 0$  from (2.22) and (2.38) below.

In the case  $V_{lm} = 0$ , which is equivalent to  $\bar{B}_{lm} = 0$ , the system (2.15)–(2.18) is overdetermined. We obtain that the parameters have to satisfy the equation

$$(d-1)l(l+1)q_u = \gamma(-f_u q_v + f_v q_u) \frac{1}{q_v} (q_u - q_v) \quad (2.29)$$

and that under this condition any eigenvalue  $\omega$  corresponding to the linearized system (2.15)–(2.18) is given by

$$-q_u \omega = \gamma(-f_u q_v + f_v q_u) + dl(l+1)q_u. \quad (2.30)$$

Due to the condition (2.29) the case  $V_{lm} = 0$  is only relevant for a small – nowhere open – subset of the parameter space. Therefore this case cannot contribute to a robust mechanism.

**2.1. Asymptotic stability with respect to spatially homogeneous perturbations.** Here we would like to consider perturbations  $u, v, V$  of a stationary state  $(u_*, v_*, V_*) \in \mathbb{R}_+^3$  such that the membrane quantities  $u, v$  are spatially homogeneous but  $V$  is allowed to be heterogeneous. We would like to characterize the stability of our system under such perturbations. In the ansatz above the restriction to spatially homogeneous  $u, v$  means that  $u_{lm} = v_{lm} = 0$  for all  $l \geq 1$ . By (2.24) and  $\psi'_{lm}(1) > 0$  (see for example [1, (10.51.5)], [16]) we deduce that also  $V_{lm} = 0$  for all  $l \geq 1$ , and in particular that  $V$  is radially symmetric. It remains to study the condition (2.27) for  $l = 0$ .

**Proposition 2.1.** *A necessary and sufficient condition for the stability of (1.1)–(1.4) in  $(u_*, v_*, V_*)$  under perturbations that are spatially homogeneous in the  $u, v$  variables is that*

$$0 < \frac{1}{3}(f_u q_v - f_v q_u) + q_V(f_v - f_u). \quad (2.31)$$

In this case

$$f_v > f_u \quad (2.32)$$

holds.

*Proof.* As remarked above we have to consider  $l = 0$ . We first restrict ourselves to the case  $V_{00} \neq 0$ . Then the system (1.1)–(1.4) is linearly asymptotically stable in  $(u_*, v_*, V_*)$  if and only if

$$\begin{aligned} G_0(\omega) = & \gamma q_V(\omega^2 + (-f_u + f_v)\gamma\omega) + \kappa_{D,0}(\omega)(\omega^2 + (-f_u + f_v)\gamma\omega) \\ & - \kappa_{D,0}(\omega)(\gamma q_v \omega - \gamma^2(f_u q_v - f_v q_u)) \end{aligned} \quad (2.33)$$

has no zeroes in  $[0, \infty)$ . Let us first consider the case  $\omega > 0$ . For convenience we then rewrite

$$\begin{aligned} \kappa_{D,0}(\omega) &= D \left( \frac{r i_0'(r)}{i_0(r)} \right) \Big|_{r=\sqrt{\frac{\omega}{D}}} = \omega \tilde{\kappa} \left( \sqrt{\frac{\omega}{D}} \right), \\ \tilde{\kappa}(r) &:= \frac{i_0'(r)}{r i_0(r)}. \end{aligned}$$

Explicit evaluation of  $\tilde{\kappa}$  gives that  $\tilde{\kappa}' < 0$ . In fact we have

$$\begin{aligned} i_0(r) &= \frac{\sinh r}{r}, \quad i_0'(r) = \frac{r \cosh r - \sinh r}{r^2}, \\ \tilde{\kappa}(r) &= \frac{r \cosh r - \sinh r}{r^2 \sinh r}, \end{aligned}$$

hence

$$\begin{aligned} \tilde{\kappa}'(r) r^3 \sinh^2 r &= -r^2 + 2 \sinh^2 r - r \sinh r \cosh r \\ &= -r^2 - 1 + \cosh 2r - \frac{r}{2} \sinh 2r \\ &= \sum_{k \geq 2} \frac{1}{(2k)!} (2r)^{2k} \left(1 - \frac{k}{2}\right) < 0. \end{aligned}$$

Furthermore we obtain

$$\lim_{r \rightarrow 0} \tilde{\kappa}(r) = \frac{1}{3}, \quad \lim_{r \rightarrow \infty} \tilde{\kappa}(r) = 0. \quad (2.34)$$

For  $\omega > 0$  the equation  $G_0(\omega) = 0$  is equivalent to

$$0 = \tilde{\kappa} \left( \sqrt{\frac{\omega}{D}} \right) \left( \omega^2 + \gamma\omega(f_v - f_u - q_v) + \gamma^2(f_u q_v - f_v q_u) \right) + \gamma q_V \omega + \gamma^2 q_V(f_v - f_u) =: \tilde{G}_0(\omega). \quad (2.35)$$

By (2.34) and  $q_V > 0$  we deduce that  $\lim_{\omega \rightarrow \infty} \tilde{G}_0(\omega) = +\infty$ . Using (2.34) we evaluate

$$\lim_{\omega \rightarrow 0} \tilde{G}_0(\omega) = \frac{1}{3} \gamma^2 (f_u q_v - f_v q_u) + \gamma^2 q_V (f_v - f_u),$$

and we obtain that

$$0 \leq \frac{1}{3}(f_u q_v - f_v q_u) + q_V(f_v - f_u). \quad (2.36)$$

is a necessary condition for  $\tilde{G}_0 > 0$  on  $(0, \infty)$ .



Let us next consider the case  $\omega = l = 0$  which gives  $G_0(0) = 0$ . In this case  $u, v, V$  are all constant and satisfy, by (2.7), (2.8) and (2.10),

$$\begin{aligned} 0 &= f_u u + f_v v, \\ 0 &= q_u u + q_v v + q_V V, \\ 0 &= 4\pi(u + v) + \frac{4\pi}{3}V. \end{aligned}$$

This system has a nontrivial solution if and only if  $0 = \frac{1}{3}(f_u q_v - f_v q_u) + q_V(f_v - f_u)$ . Together with (2.36) this property proves that (2.31) is necessary for the asserted stability.

From (2.31) we deduce that

$$0 < (f_v - f_u)(q_V - \frac{1}{3}q_v) + \frac{1}{3}(q_v - q_u)f_v \leq (f_v - f_u)(q_V - \frac{1}{3}q_v).$$

By (2.1) this implies (2.32) and in particular that (2.32) is necessary for  $\tilde{G}_0 > 0$  on  $[0, \infty)$ .

We claim that (2.31) is also sufficient to exclude a nonnegative zero of  $G_0$ . Again, we consider for  $\omega > 0$

$$\tilde{G}_0(\omega) = \tilde{\kappa} \left( \sqrt{\frac{\omega}{D}} \right) \left( \omega^2 + \gamma\omega(f_v - f_u - q_v) + \gamma^2(f_u q_v - f_v q_u) \right) + \gamma q_V \omega + \gamma^2 q_V (f_v - f_u).$$

As (2.31) implies (2.32) we have by (2.5) that  $f_v - f_u - q_v > 0$  and  $q_V(f_v - f_u) > 0$ . If we now assume

$$f_u q_v - f_v q_u > 0,$$

we immediately conclude  $\tilde{G}_0(\omega) > 0$  for all  $\omega > 0$ . If on the other hand

$$f_u q_v - f_v q_u \leq 0,$$

we remark that  $\tilde{\kappa}$  is decreasing, hence  $\tilde{\kappa} \leq \frac{1}{3}$  on  $[0, \infty)$  and therefore

$$\tilde{G}_0(\omega) > \gamma^2 \left( \frac{1}{3}(f_u q_v - f_v q_u) + q_V(f_v - f_u) \right) \geq 0$$

for all  $\omega > 0$ , which proves the claim. We have already seen above that  $0 \neq \frac{1}{3}(f_u q_v - f_v q_u) + q_V(f_v - f_u)$  is sufficient to exclude that constant perturbations  $(u, v, V)$ , corresponding to the case  $\omega = 0$ , are solution of the linearized system.

It only remains to prove that (2.31) is sufficient to exclude an instability for  $l = 0$  in the case  $V_{00} = 0$ . However, in this case by (2.29), (2.30) we have  $\omega = 0$  and we are in the case that  $(u, v, V)$  is constant, which is excluded by (2.31), as we have seen above.  $\square$

**2.2. Instability conditions.** We next characterize instabilities of our system in a spatially homogeneous stationary point  $(u_*, v_*, V_*)$  as above under general perturbations.

**Theorem 2.2.** *Assume that (2.31) is satisfied and that*

$$\begin{aligned} 0 &> (\gamma q_V + Dl)(dl^2(l+1)^2 + \gamma l(l+1)(-df_u + f_v)) \\ &\quad - D\gamma q_v l^2(l+1) + Dl\gamma^2(f_u q_v - f_v q_u) \end{aligned} \quad (2.37)$$

*holds in  $(u_*, v_*, V_*)$ . Then the system (1.1)–(1.4) is linearly asymptotically unstable in  $(u_*, v_*, V_*)$ .*

*If (2.31) and  $d = 1$  hold then (2.37) is also necessary for an instability.*

*Proof.* We again first restrict to the case  $V_{lm} \neq 0$ . Note that the right-hand side of (2.37) coincides with  $G_l(0)$  as defined in (2.27). In order to show the existence of an instability, we prove that

there is a positive zero  $\omega_{lm} > 0$  of  $G_l$ . The modified Bessel function of the first kind  $i_l$  have by [1, 10.52.1, 10.52.5], [16] the asymptotic expansions

$$i_l(r) \approx \frac{1}{2r} e^r \quad \text{as } r \rightarrow \infty, \quad i_l(r) \approx \frac{1}{(2l+1)!} r^l \quad \text{as } r \rightarrow 0.$$

This implies

$$\kappa_{D,l}(\omega) = D \left( \frac{r i'_l(r)}{i_l(r)} \right) \Big|_{r=\sqrt{\frac{\omega}{D}}} \rightarrow Dl \text{ as } \omega \rightarrow 0, \quad (2.38)$$

and  $\kappa_{D,l}(\omega) \rightarrow \infty$  as  $\omega \rightarrow \infty$  hence

$$\lim_{\omega \rightarrow \infty} G_l(\omega) = +\infty.$$

We therefore obtain that (2.37) is sufficient to guarantee a solution  $\omega > 0$  of  $G_l(\omega) = 0$ . It remains to prove that (2.37) is also necessary if  $d = 1$  holds. We will need some information on the derivative of  $\kappa_{D,l}$ . We start by observing that by (2.28)

$$\kappa'_{D,l}(\omega) = \left[ \frac{1}{2r} \left( \frac{r i'_l(r)}{i_l(r)} \right)' \right]_{r=\sqrt{\frac{\omega}{D}}}.$$

By the definition of  $i_l$  we compute

$$\frac{r i'_l(r)}{i_l(r)} = -\frac{1}{2} + \frac{r I'_{l+1/2}(r)}{I_{l+1/2}(r)}.$$

By [5] however we know that the quotient on the right-hand side has strictly positive derivative on  $\mathbb{R}^+$ . This implies that also  $\kappa'_{D,l} > 0$ . Moreover, from [7, 12] we obtain

$$\frac{r i'_l(r)}{i_l(r)} \leq l + \frac{1}{3} r^2$$

which yields

$$\kappa_{D,l}(\omega) \leq lD + \frac{1}{3}\omega = \kappa_{D,l}(0) + \frac{1}{3}\omega \quad (2.39)$$

for all  $\omega > 0$ .

This information implies by (2.27), (2.32), and  $d = 1$  that

$$\begin{aligned} G_l(\omega) &\geq \gamma q_V \left( dl^2(l+1)^2 + \gamma l(l+1)(-df_u + f_v) + (-f_u + f_v)\gamma\omega \right) \\ &\quad + \kappa_{D,l}(\omega) \left( dl^2(l+1)^2 + \gamma l(l+1)(-df_u + f_v) \right) \\ &\quad + \kappa_{D,l}(\omega) \left( -\gamma q_v(l(l+1) + \omega_{lm}) + \gamma^2(f_u q_v - f_v q_u) \right) \\ &\geq G_l(0) + \gamma^2 q_V (f_v - f_u)\omega + \gamma^2 (\kappa_{D,l}(\omega) - \kappa_{D,l}(0)) (f_u q_v - f_v q_u). \end{aligned} \quad (2.40)$$

In the case  $(f_u q_v - f_v q_u) > 0$  this yields  $G_l(\omega) \geq G_l(0)$  for all  $\omega > 0$ , as  $\kappa_{D,l}$  is increasing (see above). In the case  $(f_u q_v - f_v q_u) \leq 0$  we obtain from (2.40) that

$$G_l(\omega) \stackrel{(2.31)}{\geq} G_l(0) - \gamma^2 (f_u q_v - f_v q_u) \left( \frac{1}{3}\omega - \kappa_{D,l}(\omega) + \kappa_{D,l}(0) \right) \stackrel{(2.39)}{\geq} G_l(0).$$

for all  $\omega > 0$ . From this we conclude that  $G_l(0) < 0$  is also necessary for the existence of an instability with  $V_{lm} \neq 0$ .

It remains to consider the possibility that an instability with  $V_{lm} = 0$  exists. In this case we obtain from (2.29) and  $d = 1$  that  $-f_u q_v + f_v q_u = 0$ . But then (2.30) implies that  $\omega \leq 0$ .  $\square$

**Corollary 2.3.** *Assume (2.31). Then the instability condition (2.37) holds if the conditions of Case 1 or Case 2 below are satisfied and if  $D > 0$  is chosen sufficiently large.*

- Case 1:

$$f_u q_v - f_v q_u \geq 0, \quad (2.41)$$

$$df_u - f_v + q_v > 0, \quad (2.42)$$

$$Q := (df_u - f_v + q_v)^2 - 4d(f_u q_v - f_v q_u) > 0, \quad (2.43)$$

and there exists an  $l \in \mathbb{N}$  with

$$\lambda_- < \frac{l(l+1)}{\gamma} < \lambda_+, \quad (2.44)$$

where

$$\lambda_{\pm} = \frac{1}{2d} \left( df_u - f_v + q_v \pm \sqrt{Q} \right). \quad (2.45)$$

- Case 2:

$$f_u q_v - f_v q_u < 0 \quad (2.46)$$

and there exists an  $l \in \mathbb{N}$  with

$$\frac{l(l+1)}{\gamma} < \lambda_+, \quad (2.47)$$

where  $\lambda_+$  is as defined in (2.45).

*Proof.* In order to evaluate (2.37) for  $D \gg 1$  we consider the coefficient of  $Dl$ , that is

$$e := dl^2(l+1)^2 + \gamma l(l+1)(-df_u + f_v - q_v) + \gamma^2(f_u q_v - f_v q_u). \quad (2.48)$$

In Case 1 the last term on the left-hand side is by (2.41) nonnegative and  $e < 0$  holds if and only if the conditions (2.42)–(2.44) are satisfied.

In Case 2 the last term on the left-hand side of (2.48) is negative and  $e < 0$  holds if and only if the condition (2.47) is satisfied. Therefore  $e < 0$  holds if and only if Case 1 or Case 2 are satisfied. We now observe that the term  $Dle$  becomes dominant in (2.37) for  $D \gg 1$  and we deduce from Theorem 2.2 that if  $e < 0$  then for  $D$  sufficiently large an instability exists.  $\square$

**Remark 2.4.** (1) For  $d = 1$  we deduce from Theorem 2.2 and (2.31), (2.37) that a diffusive instability exists if and only if

$$0 > (\gamma q_v + Dl)(l^2(l+1)^2 + \gamma l(l+1)(-f_u + f_v)) - D\gamma q_v l^2(l+1) + Dl\gamma^2(f_u q_v - f_v q_u)$$

holds. By (2.32) we deduce that (2.46) is necessary and that only Case 2 is a possible scenario for an instability. By Corollary 2.3 this condition and (2.47) for an  $l \in \mathbb{N}$  are also sufficient to ensure, for  $D$  sufficiently large, an instability. In particular, for  $d = 1$  there exist parameter values such that the system has a diffusive instability.

(2) Assume (2.31). Then we observe from (2.27) that perturbations in directions of eigenvectors  $\varphi_{lm}$  decay for all sufficiently large  $l \in \mathbb{N}$ .

(3) Case 1 or Case 2 in Corollary 2.3 are sufficient but not necessary for an instability. A third case may arise for  $d \gg 1$  and  $D$  sufficiently small. In fact, even if the factor that multiplies  $\kappa_{D,l}(\omega)$  in (2.27) is positive, this term might be dominated by the first line in (2.27), which becomes negative if  $df_u - f_v \gg 1$ . As we are mostly interested in  $d = 1$  we do not investigate this case further.

**Remark 2.5.** We finally would like to relate the distinction between Case 1 and Case 2 instabilities, given by the inequalities (2.41) and (2.46), to the stability properties of the zero lateral diffusion reduction of the full system (1.1)–(1.4). This reduction is given by choosing  $d_u = d_v = 0$

in the dimensional formulation of our system, see (A.10) and (A.11) in the appendix and leads to the system

$$\partial_t V = D\Delta V \quad \text{in } B \times I, \quad (2.49)$$

$$\partial_t u = \gamma f(u, v) \quad \text{on } \Gamma \times I, \quad (2.50)$$

$$\partial_t v = \gamma(-f(u, v) + q(u, v, V)) \quad \text{on } \Gamma \times I, \quad (2.51)$$

$$-D\nabla V \cdot \nu = \gamma q(u, v, V) \quad \text{on } \Gamma \times I. \quad (2.52)$$

An instability of the corresponding system is then characterized by the existence of a positive root  $\omega_{lm}$  of

$$0 = \gamma q_V (\omega_{lm}^2 + (-f_u + f_v)\gamma\omega_{lm}) + \kappa_{D,l}(\omega_{lm}) \left( \omega_{lm}^2 + (-f_u + f_v - q_v)\gamma\omega_{lm} + \gamma^2(f_u q_v - f_v q_u) \right) \quad (2.53)$$

with  $\kappa_{D,l}$  as in (2.28). We therefore see that under the stability assumption (2.31) in Case 1, i.e. if (2.41) holds, the system (2.49)–(2.52) is stable, whereas for Case 2, i.e. if (2.46) holds, the system is unstable for  $D \gg 1$  and  $\gamma$  chosen large enough. This shows that the second instability mechanism is not induced by the membrane diffusion but rather by the cytosolic diffusion. See Section 6 for a further discussion.

### 3. STABILITY ANALYSIS FOR THE NON-LOCAL REDUCTION $D \rightarrow \infty$

By formally letting  $D \rightarrow \infty$  in (1.1)–(1.4) one obtains the following reduced two-variable system

$$\partial_t u = \Delta_\Gamma u + \gamma f(u, v), \quad (3.1)$$

$$\partial_t v = d\Delta_\Gamma v + \gamma(-f(u, v) + q(u, v, V[u + v])), \quad (3.2)$$

where  $V[u + v]$  is the *non-local* functional

$$V[u + v] = V_{init} - c \int_\Gamma (u + v) d\sigma, \quad (3.3)$$

with  $V_{init} > 0$  given and  $c := \frac{1}{|B|}$ . Note that  $V_{init}$  is determined by the total mass of GTPase, which is constant in time. The system (3.1)–(3.3) has already been considered in [17] and has, compared to the fully coupled system, the advantage of having one fixed domain of definition (the membrane  $\Gamma$ ). The remnant of the spatial coupling in the full system is the non-locality, introduced by the specific form of  $V = V[u + v]$ . In [17] we have, among other things, presented a stability analysis, which however was not complete in the characterization of instabilities [19]. Here we complete that discussion and obtain a characterization that coincides with the behavior of (1.1)–(1.4) for large cytosolic diffusion constant  $D$ . Moreover we obtain some additional properties of instabilities that are more difficult to characterize for the fully coupled system.

In the following stability analysis, in contrast to the one of the full system, we do not need to restrict ourselves to spherical cell shapes. We therefore fix an arbitrary open, bounded domain  $B \subset \mathbb{R}^3$  with smooth connected boundary  $\Gamma = \partial B$ . We assume again that  $f$  and  $q$  satisfy (2.1), consider a spatially homogeneous stationary point  $(u_*, v_*)$  of (3.1)–(3.3), and set  $V_* := V[u_*, v_*]$ . Then  $(u_*, v_*)$  is also a stationary point of the ODE reduction of (3.1), (3.3),

$$\partial_t u = \gamma f(u, v), \quad (3.4)$$

$$\partial_t v = \gamma(-f(u, v) + q(u, v, V_1(u + v))), \quad (3.5)$$

where

$$V_1(u + v) = V_{init} - c|\Gamma|(u + v).$$

Note that  $V_1$  is just a (non-local) real function and that  $V_1' = -c|\Gamma| < 0$ . Again it is convenient to introduce the notation

$$\begin{aligned} f_u &:= \partial_u f(u_*, v_*), & f_v &:= \partial_v f(u_*, v_*), \\ q_u &:= \partial_u q(u_*, v_*, V_*) & q_v &:= \partial_v q(u_*, v_*, V_*), & q_V &:= \partial_V q(u_*, v_*, V_*). \end{aligned}$$

The stability of the ODE system (3.4), (3.5) in  $(u_*, v_*)$  is equivalent to the conditions

$$0 > f_u - f_v + q_v + q_V V_1', \quad (3.6)$$

$$0 < f_u(q_v + q_V V_1') - f_v(q_u + q_V V_1'). \quad (3.7)$$

This also corresponds to the stability of (3.1), (3.2) in  $(u_*, v_*)$  with respect to spatially homogeneous perturbations. We remark that (2.1) and (3.7) imply that

$$\begin{aligned} 0 &< f_u q_v - f_v q_u + q_V V_1' (f_u - f_v) = (f_u - f_v)(q_v + q_V V_1') + f_v(q_v - q_u) \\ &\leq (f_u - f_v)(q_v + q_V V_1'), \end{aligned}$$

which by (2.1) yields that

$$f_u < f_v. \quad (3.8)$$

In particular we see that under the assumption (2.1) the inequality (3.7) already implies (3.6).

We remark that (3.7) coincides in the case of a spherical cell, i.e.  $\Gamma = S^2 \subset \mathbb{R}^3$  with the stability condition (2.31) for  $D < \infty$ . In fact, in this case we have  $c|\Gamma| = \frac{4\pi}{4\pi/3} = 3$  and we obtain for the right-hand side in (3.7) that

$$f_u(q_v + q_V V_1') - f_v(q_u + q_V V_1') = f_u q_v - f_v q_u - 3q_V(f_u - f_v)$$

and the equivalence of (3.7) and (2.31) follows.

For the instability of (3.1)–(3.2) in  $(u_*, v_*)$  we obtain the following characterization.

**Proposition 3.1.** *Assume that conditions (2.1) and (3.6), (3.7) hold. Then the system (3.1), (3.2) is unstable in  $(u_*, v_*)$  if and only if in this point either the conditions from Case 1 or Case 2 below are satisfied:*

- Case 1:

$$f_u q_v - f_v q_u \geq 0, \quad (3.9)$$

$$df_u - f_v + q_v > 0, \quad (3.10)$$

$$Q := (df_u - f_v + q_v)^2 - 4d(f_u q_v - f_v q_u) > 0,$$

and there exists an eigenvalue  $\mu > 0$  of  $-\Delta_\Gamma$  with

$$\lambda_- < \frac{\mu}{\gamma} < \lambda_+,$$

where

$$\lambda_\pm = \frac{1}{2d} \left( df_u - f_v + q_v \pm \sqrt{Q} \right). \quad (3.11)$$

- Case 2:

$$f_u q_v - f_v q_u < 0 \quad (3.12)$$

and there exists an eigenvalue  $\mu > 0$  of  $-\Delta_\Gamma$  with

$$\frac{\mu}{\gamma} < \lambda_+, \quad (3.13)$$

where  $\lambda_+$  is as defined in (3.11).

*Proof.* The linearization of (3.1), (3.2) in  $(u_*, v_*)$  is given by

$$\partial_t u = \Delta_\Gamma u + \gamma f_u u + \gamma f_v v, \quad (3.14)$$

$$\partial_t v = d\Delta_\Gamma v + \gamma \left( -f_u u - f_v v + q_u u + q_v v - c q_V \int_\Gamma (u + v) d\sigma(x) \right). \quad (3.15)$$

It suffices to consider perturbations of the form

$$u(y, t) = a e^{\omega t} \psi(y), \quad v(y, t) = b e^{\omega t} \psi(y) \quad (3.16)$$

with  $a, b \in \mathbb{R}$ , where  $\psi$  is an eigenvector of  $-\Delta_\Gamma$  to an eigenvalue  $\mu$ . The operator  $-\Delta_\Gamma$  has only countably many eigenvalues that are nonnegative. Zero is a simple eigenvalue with eigenspace given by the constant functions on  $\Gamma$ . As we have considered spatially homogeneous perturbations already above we can restrict ourselves to  $\mu > 0$ . Any eigenvector for an eigenvalue  $\mu > 0$  satisfies

$$\int_\Gamma (u + v) d\sigma(x) = 0.$$

Then  $(u, v)$  as in (3.16) is a solution of (3.14), (3.15) if and only if

$$\begin{aligned} 0 = & \omega^2 + \omega((d+1)\mu + \gamma(-f_u + f_v - q_v)) \\ & + d\mu^2 + \gamma\mu(-df_u + f_v - q_v) + \gamma^2(f_u q_v - f_v q_u). \end{aligned} \quad (3.17)$$

The inequality (3.8) implies that in (3.17) the term on the right-hand side that is linear in  $\omega$  is positive for positive  $\omega$ . A positive zero of this equation therefore exists if and only if

$$d\mu^2 + \gamma\mu(-df_u + f_v - q_v) + \gamma^2(f_u q_v - f_v q_u) < 0. \quad (3.18)$$

which is identical to (2.48) for  $\mu = l(l+1)$ . In Corollary 2.3 we have proved that this condition is equivalent to the property that Case 1 or Case 2 hold.  $\square$

By Proposition 3.1 the (sufficient) instability conditions from Corollary 2.3 are sharp for  $D = \infty$ . We remark that in the classical local case, which corresponds to  $q_V = 0$ , by (3.7) only Case 1 is possible, which just describes the usual conditions for a Turing instability. Case 2 on the other hand represents a different mechanism that is not present for local two-variable systems.

Similarly as in Remark 2.5 we observe for the non-local system (3.1)–(3.3) that the inequality (3.9) that characterizes Case 1 corresponds to the stability of the non-local ODE system (3.4), (3.5) with respect to spatially heterogeneous perturbations. Due to the non-locality this property however is not equivalent to the stability of the non-local reaction–diffusion system with respect to spatially homogeneous perturbations. In particular, even for zero lateral diffusion in the case that (3.12), (3.13) hold the non-local system is unstable with respect to spatially heterogeneous perturbations. See Section 6 for a further discussion.

In Case 1 we deduce from (3.10) that  $f_u > 0$  and further, by (2.1) and (3.9)

$$0 \leq f_u q_v - f_v q_u \leq (f_u - f_v) q_u,$$

hence  $q_u \leq 0$ . In particular, in Case 1 the stationary point  $(u_*, v_*)$  needs to be of activator–substrate-depletion type. In contrast Case 2 is less restrictive, and does allow for stationary points with  $f_u \leq 0$  and  $q_u \geq 0$ .

We further observe that for equal lateral diffusion  $d = 1$  no instabilities of (3.1), (3.2) exist in Case 1. In fact (3.8), (3.10), and (2.1) would imply

$$0 > f_u - f_v > -q_v \geq 0,$$

which gives a contradiction. In contrast, in Case 2, i.e. under the condition (3.12), for any  $d \geq 0$  there exists  $\gamma > 0$  such that (3.13) is satisfied and an instability exists.

A particular property, different from the classical Turing instability is that for  $d = 1$  in Case 2 the most unstable perturbations of system (3.1), (3.2) is always in direction of an eigenvector corresponding to the smallest positive eigenvalue  $\mu$ . In fact, if we consider the unique positive

root  $\omega = \omega(\mu)$  of (3.17) as function of  $\mu > 0$  we observe that  $\omega(\mu) + \mu$  is independent of  $\mu$  and we therefore deduce that  $\omega(\mu)$  is decreasing in  $\mu$ .

#### 4. NUMERICAL TREATMENT OF THE FULL SYSTEM

In the following, we present numerical simulations of (1.1)–(1.4). These confirm the results of the linear stability analysis of Section 2 and in addition allow to study the behavior beyond the linear regime.

**4.1. Phase-field approach for coupling bulk- and surface PDE's.** In order to numerically treat equations on the membrane and inside the cell, we use a phase-field approach. A diffuse-interface description of coupled bulk diffusion and ordinary differential equations on the bounding surface has been proposed in [13] to simulate membrane-bound Turing patterns. In [18] a diffuse-interface approach for solving PDE's on surfaces has been introduced. Moreover, in [14] a diffuse-interface approximation for PDE's in domains with boundaries implicitly given by phase field functions has been provided, see also [11] for the special case of no-flux boundary conditions. In order to treat the spatially coupled system (1.1)–(1.4) we combine both methods. For a similar approach see [20]. Alternative methods, different from a phase-field approach have also been used in similar contexts. A finite element analysis for a coupled bulk–surface equation has recently been presented in [3]. In [15] finite volume techniques are applied to reaction–diffusion equations on curved surfaces, coupled to diffusion in the volume.

We use here the diffuse-interface approach as a convenient numerical method. It can more easily be adapted to complicated domains and realistic cell shapes. In this case the main effort is to construct a suitable discrete signed-distance function from the cell boundary, which is often easier to obtain than a triangulation of the boundary, necessary in other methods. Furthermore, coupling of equations in the bulk and on its boundary does not require any coupling of meshes with different dimensions. Finally, an extension of the phase-field approach to evolving membrane shapes is in principle relatively easy (though costly) and even allows to include topological changes. On the other hand, solving partial differential equations on  $\Gamma$  is computationally certainly more expensive in a diffuse-interface setting.

The strategy of the phase-field approach is as follows: We choose a (simple) computational domain  $\Omega$  containing  $\bar{B}$  and we introduce a smeared-out indicator function  $\phi : \Omega \rightarrow \mathbb{R}$ , for example given by

$$\phi(x) := \frac{1}{2}(1 - \tanh(3r(x)/\varepsilon)),$$

where  $r$  denotes the signed distance from  $\Gamma$ , chosen negative inside  $B$  and positive outside  $\bar{B}$ . The surface  $\Gamma$  is then given by the level set  $\{\phi = \frac{1}{2}\}$ . The corresponding ‘diffuse interface’ is understood as the layer where  $\phi$  is away from  $\pm 1$ . The order of the diffuse interface width is then determined by the (small) parameter  $\varepsilon > 0$ .

We define  $b(z) := 36z^2(z - 1)^2$  for  $z \in \mathbb{R}$ . According to [18] and [14], a diffuse-interface approximation for the coupled system (1.1)–(1.4) is given by

$$\phi \partial_t V = D \nabla \cdot (\phi \nabla V) - \varepsilon^{-1} b(\phi) \gamma q(u, v, V), \quad (4.1)$$

$$b(\phi) \partial_t u = \nabla \cdot (b(\phi) \nabla u) + b(\phi) \gamma f(u, v), \quad (4.2)$$

$$b(\phi) \partial_t v = d \nabla \cdot (b(\phi) \nabla v) + b(\phi) \gamma (-f(u, v) + q(u, v, V)) \quad (4.3)$$

for unknown functions  $u, v, V : \Omega \times I \rightarrow \mathbb{R}$ . We complement this system by initial conditions

$$V(\cdot, 0) = V_0, \quad v(\cdot, 0) = v_0, \quad u(\cdot, 0) = u_0$$

for given extensions to  $\Omega$  of the original initial conditions  $u_0, v_0, V_0$ , which were only defined on  $\Gamma$  and  $B$ , respectively. In (4.1) the phase field function  $\phi$  restricts the time derivative and diffusion to the cell, while the function  $b(\phi)$  restricts the flux  $q$  to the membrane. Accordingly, in (4.2), (4.3) the function  $b(\phi)$  is applied to restrict the reaction diffusion equations to the membrane.

**4.2. Numerical Approach.** We consider either the sphere  $\Gamma = S^2$  or an ellipsoid  $\Gamma$  with semi-axes  $a, b$  and  $c$  in  $x_1$ -,  $x_2$ - and  $x_3$ -direction, respectively. To discretize in time we use a semi-implicit Euler scheme with all nonlinearities linearized corresponding to a single Newton step. We choose a computational domain  $\Omega := (-2, 2)^3$  containing  $\bar{B}$ , and we use an adaptively refined mesh in order to discretize system (4.1)–(4.3) in space using linear finite elements. On the boundary  $\partial\Omega$  we assume periodicity of the discrete solutions  $u_h, v_h, V_h$ . Due to the degeneracy of equations (4.1)–(4.3) and to avoid numerical problems we regularize (4.1)–(4.3) in all second order terms by adding a small positive number  $\delta$  to  $b(\phi)$ . The resulting linear system of equations is solved by a stabilized bi-conjugate gradient method (BiCGStab) for  $(u_h, v_h, V_h)$  in each time step. The resulting scheme has been implemented in the adaptive FEM toolbox AMDiS [21].

**4.3. Numerical Examples.** In all computations, we use  $f, q$  as given in (A.10) and (A.11), respectively. We assume random initial conditions  $u_0 : \Omega \rightarrow [0, 0.0002]$ ,  $v_0 : \Omega \rightarrow [0, 0.0002]$ . Moreover, we choose a constant initial condition  $V_0$  for  $V_h$  such that the expected value of the total mass in the system is given by  $V_{init}|B|$  and  $V_{init} = 5.1$ , which is the value used in Section 5 for the reduced system. This choice results in the case of a spherical cell in the initial condition  $V_0 = 5.0994$  for the cytosolic concentration  $V_h$ .

For the parameters that determine  $f$  and  $q$  in (A.10), (A.11) we chose the values given in Table 1. In particular we always assume  $d = 1$  corresponding to equal lateral diffusion constants for  $u$  and  $v$ . Note that for this choice, Case 2 in Corollary 2.3 applies and guarantees an instability for  $D > 0$  sufficiently large.

parameter	$d$	$\gamma$	$a_1$	$a_2$	$a_3$	$a_4$	$a_5$	$a_6$	$a_{-6}$	$\varepsilon$	$\delta$
value	1	400	0.02	20	160	1	0.5	0.36	5	0.1	$10^{-6}$

TABLE 1. Parameters used for numerical results.

**4.3.1. Instability for large cytosolic diffusion coefficient.** First, we choose  $D = 100$ . In Fig. 1 we see results in this case, showing contour plots of the solutions  $u_h, v_h, V_h$  evaluated on the level set  $\Gamma_h := \{\phi_h = 1/2\}$  at different times. Thereby, one observes the evolution to an unstable stationary solution and towards an equilibrium with local maxima of  $u_h$  and  $v_h$  on  $\Gamma_h$ . In a way this result shows similarities to Turing-type instabilities, where usually differences in diffusion constants drive the instability. In this case,  $d = 1$  corresponds to equal lateral diffusion constants. However, the large cytosolic diffusion admits the development of heterogeneities.

**4.3.2. Stability for equal lateral and cytosolic diffusion coefficients.** For  $D = d = 1$ , there is no instability as the results in Fig. 2 indicate.

**4.3.3. Ellipsoidal membrane.** We consider an ellipsoidal membrane  $\Gamma$  with semi-axes 0.75, 1 and 1.5. As in the first example we have used  $D = 100$ . In Fig. 3, the evolution towards a nearly stationary discrete solution  $u_h$  on the level set  $\{\phi_h = \frac{1}{2}\}$  is displayed.

## 5. NUMERICAL TREATMENT OF THE NON-LOCAL SYSTEM

In this section, we use a parametric finite element description of the non-local system (3.1)–(3.3) in order to numerically investigate instabilities for  $d = 1$  found in Sec. 3. For this purpose, we apply the algorithm described in [17]. To discretize in time, we apply a semi-implicit Euler scheme, where all nonlinearities are linearized in a suitable way. We use a parametric finite element approach [2] with linear finite elements, where we solve as a system for the two concentrations  $u, v$  on the membrane. The non-local term is treated fully explicitly. The resulting linear system is solved by a stabilized bi-conjugate gradient method (BiCGStab). The scheme is implemented using the adaptive finite element toolbox AMDiS [21].



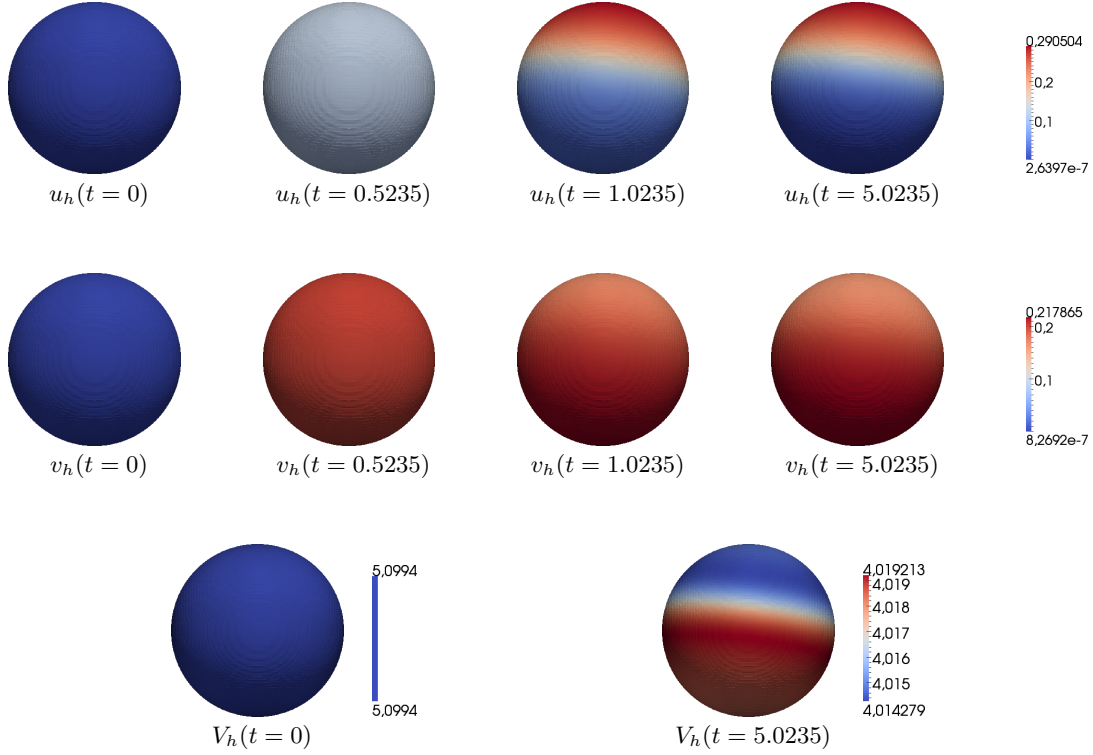


FIGURE 1. Instability for increased cytosolic diffusion ( $D = 100$ ). From left to right: the discrete solutions  $u_h$  (upper row),  $v_h$  (middle row) on level set  $\{\phi_h = \frac{1}{2}\}$  for  $t = 0, t = 0.5235, t = 1.0235$ , and  $t = 5.0235$ , discrete solution  $V_h$  on level set  $\{\phi_h = \frac{1}{2}\}$  for  $t = 0, t = 5.0235$  (lower row).

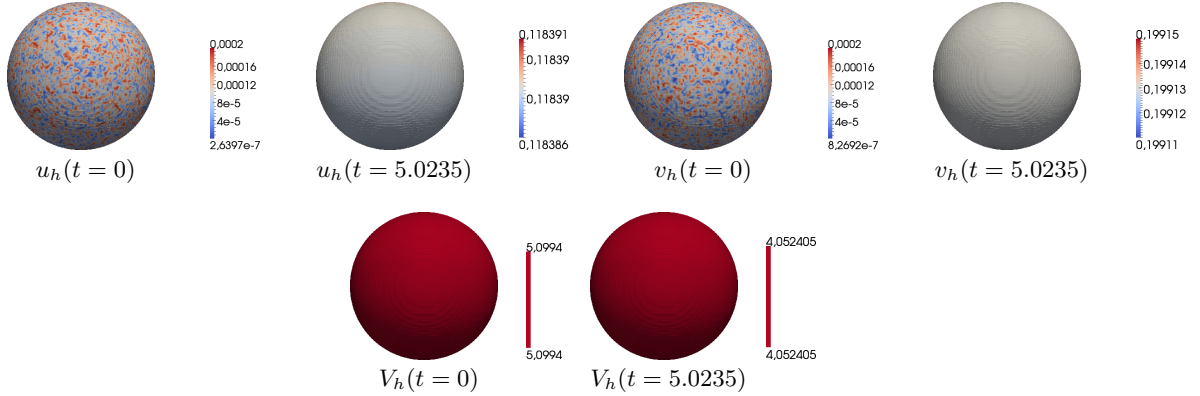


FIGURE 2. Stability for equal membrane and cytosolic diffusion coefficients ( $D = 1$ ). From left to right: The discrete initial and stationary solutions  $u_h$ ,  $v_h$  and  $V_h$  on level set  $\{\phi_h = \frac{1}{2}\}$ .

**5.1. Numerical Examples.** In all following examples we use for  $f$  and  $q$  the specific choices proposed in (A.10) and (A.11), respectively. Thereby, we use parameters from Table 2. Furthermore, we consider the unit-sphere  $\Gamma = S^2$  and its discrete approximation  $\Gamma_h$  through a triangulation with a uniform grid. We assume random initial conditions  $u_0 : \Gamma_h \rightarrow [0, 0.0002]$ ,  $v_0 : \Gamma_h \rightarrow [0, 0.0002]$ . Moreover, we choose  $V_{init} = 5.1$ . Note that this choice of initial conditions is the exact counterpart of the initial conditions used for the simulation of the full system in Section 4.

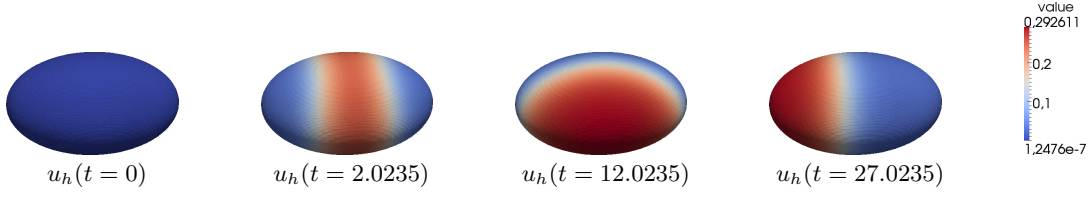


FIGURE 3. Instability for increased cytosolic diffusion ( $D = 100$ ). From left to right: the discrete solutions  $u_h$  on level set  $\{\phi_h = \frac{1}{2}\}$  for  $t = 0$ ,  $t = 2.0235$ ,  $t = 12.0235$ , and  $t = 27.0235$ .

parameter	$d$	$\gamma$	$a_1$	$a_2$	$a_3$	$a_4$	$a_5$	$a_6$	$a_{-6}$
value	1	400	0.02	20	160	1	0.5	0.36	5

TABLE 2. Parameters used for numerical results (non-local model).

5.1.1. *Instability with equal lateral diffusion coefficients.* In Fig. 4, one can see contour plots of the discrete solutions  $u_h, v_h$  at different times for  $d = 1$ . Similarly to the first example in Sec. 4, one observes an evolution to an unstable spatially homogeneous solution and towards a stationary solution with a single spot pattern, which is in agreement with remarks in Sec. 3.

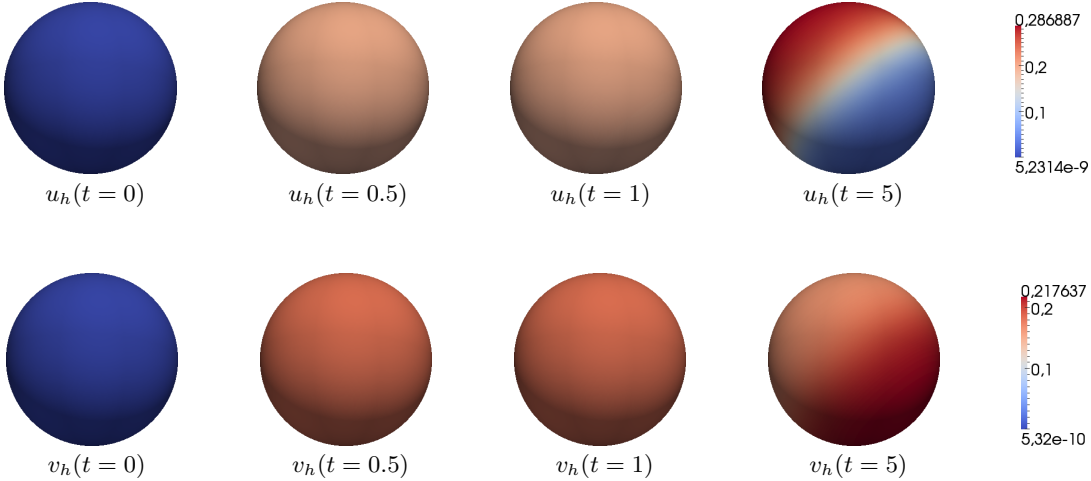


FIGURE 4. Instability with diffusion ( $d = 1$ ). From left to right: the discrete solutions  $u_h$  (upper row),  $v_h$  (lower row) for  $t = 0$ ,  $t = 0.5$ ,  $t = 1$ , and  $t = 5$ .

5.1.2. *Stability for increased diffusion.* For increased diffusion coefficient, the instability vanishes, see Fig. 5. Here we have scaled  $f, q$  and time  $t$  by a factor  $1/10$ , which corresponds to scaling the diffusion coefficients  $d_u$  and  $d_v$  in the dimensional formulation (see the appendix) by a factor 10. To be more precise, we have decreased the value of  $\gamma$  from 400 as in Table 2 to 40 and have rescaled time. The explanation for the stabilization by lowering the value of  $\gamma$  is that the inequality (2.47) is violated for small enough  $\gamma$ . In an informal way one could explain this effect as a consequence of the ‘decreased difference’ between cytosolic diffusion constant  $D = \infty$  and lateral membrane diffusions  $d_u, d_v$ . This suggests, that for  $d_u = d_v$  and an Case 2 instability large differences between  $D$  and  $d_u, d_v$  are required, which resembles a classical Turing type mechanism in the  $V, u$  variables.

5.1.3. *Rich Nonlinear Dynamics.* In Fig. 6, we present results showing the rich dynamics the model includes. Thereby we replace the corresponding parameters in Table 1 by the values

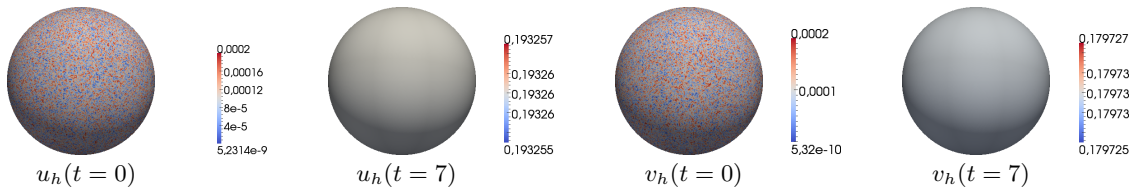


FIGURE 5. Stability for increased diffusion: The discrete initial and stationary solutions  $u_h$  (left),  $v_h$  (right).

given in Table 3. One observes that the system evolves to a homogeneous stationary which is unstable and later forms a pattern, which is again unstable. Finally the system reaches a stable homogenous stationary state, different from the initial one.

parameter	$d$	$\gamma$	$a_1$	$a_2$	$a_3$	$a_4$	$a_5$	$a_6$	$a_{-6}$	$V_{init}$
value	1	2000	0.001	20	160	1	0.5	0.36	10.3757	10.1

TABLE 3. Parameters used for numerical results in Fig. 6.

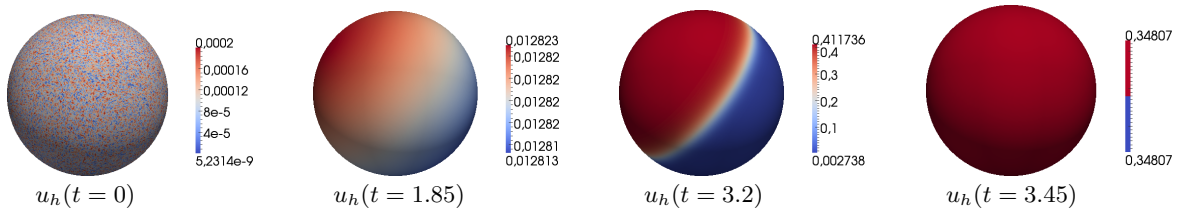


FIGURE 6. Rich nonlinear dynamics for different set of parameters: discrete solution  $u_h$  at initial time, at  $t = 1.85$  showing an unstable intermediate solution, at  $t = 3.2$  with an intermediate pattern and homogenous stationary solution.

## 6. DISCUSSION

We have analytically and numerically studied a coupled system of surface–bulk reaction–diffusion equations. Such a system for example arises in [17] as a model for the GTPase cycle in biological cells. Here the relevant quantities are the concentrations  $u, v$  of active and inactive GTPase on the membrane, and the concentration  $V$  of inactive GTPase in the cytosolic volume. Our main interest here was to analyze the possibility of a symmetry breaking. The latter refers to an instability of spatially homogeneous stationary points that are stable with respect to symmetry-conserving perturbations, which in our case means that  $u, v$ , and the boundary values of  $V$  are spatially homogeneous.

For spherical cell shapes we have performed a linearized stability analysis and have discovered that two different mechanisms for symmetry breaking are present. The first one requires a large difference in the lateral diffusion constants of  $u$  and  $v$ , expressed by a large value of  $d$  in (1.1)–(1.4). This mechanism is closely related to a classical Turing instability for a two-variable system with  $u$  as activator and  $v$  as substrate. The second mechanism however does even occur for equal lateral diffusion constants of  $u$  and  $v$ , i.e. even for  $d = 1$ , which is much more realistic in the application to the GTPase cycle in cells. This second mechanism on the other hand requires that the cytosolic diffusion coefficient  $D$  is much larger than the lateral diffusion coefficients. The simulations show that a factor of 100 between both is sufficient, which is about the ratio between cytosolic and lateral membrane diffusion measured for biological cells [10]. The new

second instability mechanism is much closer to a Turing type mechanism in the  $V, u$  variables and is a specific property of coupled surface–bulk reaction–diffusion systems.

Our results for the fully coupled system are comparable to those for its non-local reduction in the infinite cytosolic diffusion limit. However, here the corresponding stability analysis applies to more general membrane shapes and the reduction allows to further illuminate the two instability mechanisms. We in particular observe that for  $d = 1$  in the new second mechanism the most unstable perturbation is always in direction of eigenvectors corresponding to the smallest nonzero eigenvalue. This prefers the formation of a single membrane component with high concentration of activated GTPase. Again, this is much more in coincidence with the experimentally observed behavior than a classical Turing mechanism, where the emerging patterns are typically very sensitive to parameter changes. We remark that the same robust localization into a single spot has also been observed in [4] in a related model for the GTPase cycle.

The distinction between the two mechanisms is expressed by the inequalities (2.41) and (2.46). As observed in Remark 2.5 the latter implies that for Case 2 instabilities the spatially homogeneous state is unstable with respect to spatially heterogeneous perturbations even in the absence of membrane diffusion. It is important to notice that in the full and in the reduced model there is a difference between (a) the stability with respect to perturbations that are spatially homogeneous on the cell membrane (and radially symmetric in the cell), and (b) the stability (with respect to not necessarily spatially homogeneous perturbations) of the corresponding systems without membrane diffusion. For local reaction–diffusion systems such a difference is not present and there is a coincidence between diffusive instabilities and symmetry breaking. Since for our models and a Case 2 instability the symmetric state is even without membrane diffusion unstable the term ‘diffusion induced instability’ might appear inappropriate. On the other hand, as explained above, the instability originates from the large cytosolic diffusion compared to the lateral diffusion and is in this respect diffusion induced. The main property of both a Case 1 and a Case 2 instability is that we observe a symmetry breaking, which is clearly confirmed by our numerical simulations. Starting from a spatially homogeneous distribution, as long as no stationary point is reached, the system is driven by the kinetic reaction and sorption terms and spatial heterogeneities are not amplified. If the evolution approaches a homogeneous stationary state (and this typically requires its stability with respect to spatially homogeneous perturbations) and if this state is unstable with respect to general perturbations then heterogeneous patterns develop and a symmetry breaking occurs. When the evolution moves away from the stationary point the nonlinear effects again come into play and determine the long-time behavior.

#### APPENDIX A. NON-DIMENSIONALIZATION

Here we recall the formulation of the reaction–diffusion model for the GTPase cycle proposed in [17]. We give specific choices of reaction and attachment/detachment laws, and the dimensional formulation including all physical units.

As above we denote the cytosolic volume of a cell by  $B$  and the cell membrane by the boundary  $\Gamma = \partial B$  of  $B$ , which is assumed to represent a smooth, closed two-dimensional surface. In addition, we fix a time interval of observation  $I$ . We formulate a system of reaction–diffusion equations for the unknowns

- $V$  concentration of cytosolic GDP-GTPase (in complex with GDI),
- $v$  concentration of membrane-bound GDP-GTPase,
- $u$  concentration of membrane-bound GTP-GTPase.

Physical units are given by

$$[V] = \frac{\text{mol}}{\text{m}^3}, \quad [u] = [v] = \frac{\text{mol}}{\text{m}^2}.$$

The following specific form was proposed in [17],

$$\partial_t V = D\Delta V \quad \text{in } B \times I, \quad (\text{A.1})$$

$$\partial_t u = d_u \Delta_\Gamma u + k_1 v g_0 \left(1 - \frac{K_5 u}{1 + K_5 u}\right) + k_2 v \frac{K_5 u g_0}{1 + K_5 u} - k_3 \frac{u}{u + k_4} \quad \text{on } \Gamma \times I, \quad (\text{A.2})$$

$$\partial_t v = d_v \Delta_\Gamma v - k_1 v g_0 \left(1 - \frac{K_5 u}{1 + K_5 u}\right) - k_2 v \frac{K_5 u g_0}{1 + K_5 u} + k_3 \frac{u}{u + k_4} + q \quad \text{on } \Gamma \times I \quad (\text{A.3})$$

together with a constitutive law for attachment/detachment kinetics and a flux condition,

$$-D\nabla V \cdot \nu = q \quad \text{on } \Gamma, \quad (\text{A.4})$$

$$q = b_6 \frac{|B|}{|\Gamma|} V (c_{\max} - u - v)_+ - b_{-6} v. \quad (\text{A.5})$$

The partial differential equations (A.1)–(A.3) include kinetic rates  $k_i$ ,  $i \in \{1, 2, 3, 4\}$ ,  $K_5$  and an equilibrium concentration of membrane-bound GEF  $g_0$  with units

$$[k_1] = [k_2] = \frac{\text{m}^2}{\text{mol} \cdot \text{s}}; \quad [k_3] = \frac{\text{mol}}{\text{m}^2 \cdot \text{s}}; \quad [k_4] = \frac{\text{mol}}{\text{m}^2}; \quad [K_5] = \frac{\text{m}^2}{\text{mol}}; \quad [g_0] = \frac{\text{mol}}{\text{m}^2}.$$

Furthermore, we have units of diffusion coefficients  $D, d_u, d_v$  and sorption coefficients  $b_6, b_{-6}$  given by

$$[D] = [d_u] = [d_v] = \frac{\text{m}^2}{\text{s}}; \quad [b_6] = \frac{\text{m}^2}{\text{mol} \cdot \text{s}}; \quad [b_{-6}] = \frac{1}{\text{s}}.$$

In (A.4),  $\nu$  denotes the outward unit normal to  $B$  at  $\Gamma$ . The constitutive equation (A.5) for the flux  $q$  includes a saturation value  $c_{\max}$ . Membrane attachment is treated as a reaction between cytosolic GTPase and a free site on the membrane and modeled by a Langmuir rate law [9]. Detachment is taken proportional to the inactive GTPase concentration.

In order to obtain a non-dimensional model, we follow [17] and define dimensionless spatial and time coordinates

$$\xi := \frac{1}{R} x; \quad \tau := \frac{d_u}{R^2} t,$$

where  $R > 0$  denotes a typical length. We define  $\gamma > 0$  through  $R = \sqrt{\gamma} \mathbb{I}$  with  $\mathbb{I} = 1\text{m}$  denoting the unit length. This leads to transformed domain  $\tilde{B} := \{\xi \in \mathbb{R}^3 : R\xi \in B\}$ ,  $\tilde{\Gamma} := \partial\tilde{B}$  and time interval  $\tilde{I} := \{\tau \in \mathbb{R} : \frac{R^2\tau}{d_u} \in I\}$ . Non-dimensional concentrations are defined through

$$\tilde{V} := \frac{R}{c_{\max}} V, \quad \tilde{u} := \frac{1}{c_{\max}} u, \quad \tilde{v} := \frac{1}{c_{\max}} v.$$

Moreover, we introduce dimensionless quantities

$$a_1 := \frac{\mathbb{I}^2}{d_u} k_1 g_0, \quad a_2 := \frac{1}{K_5 c_{\max}}, \quad a_3 := \frac{k_2}{k_1} a_1, \quad a_4 := \frac{\mathbb{I}^2}{d_u c_{\max}} k_3, \quad a_5 := \frac{k_4}{c_{\max}},$$

$$a_6 := \frac{\mathbb{I}^2 b_6}{d_u c_{\max}} \frac{|B|}{|\Gamma| R}, \quad a_{-6} := \frac{\mathbb{I}^2 b_{-6}}{d_u}, \quad d := \frac{d_v}{d_u}, \quad \tilde{D} := \frac{D}{d_u}.$$

With these definitions, dropping all tildes and replacing  $\xi$  and  $\tau$  by  $x$  and  $t$ , respectively, we arrive at the full mathematical model [17]

$$\partial_t V = D\Delta V \quad \text{in } B \times I, \quad (\text{A.6})$$

$$\partial_t u = \Delta_\Gamma u + \gamma f(u, v) \quad \text{on } \Gamma \times I, \quad (\text{A.7})$$

$$\partial_t v = d\Delta_\Gamma v + \gamma(-f(u, v) + q(u, v, V)) \quad \text{on } \Gamma \times I \quad (\text{A.8})$$

with the flux condition

$$-D\nabla V \cdot \nu = \gamma q \quad \text{on } \Gamma \times I, \quad (\text{A.9})$$

where

$$f(u, v) := \left( a_1 + (a_3 - a_1) \frac{u}{a_2 + u} \right) v - a_4 \frac{u}{a_5 + u}, \quad (\text{A.10})$$

$$q(u, v, V) := a_6 V (1 - (u + v))_+ - a_{-6} v. \quad (\text{A.11})$$

We remark that for  $a_1 < a_3$ , which is again a natural assumption (see [17]), all the properties that we have assumed in (2.1) are satisfied.

## REFERENCES

- [1] *NIST Digital Library of Mathematical Functions*. <http://dlmf.nist.gov/>, Release 1.0.5 of 2012-10-01. <http://dlmf.nist.gov/>. – Online companion to [16]
- [2] DZIUK, G. ; ELLIOTT, C. M.: Surface Finite Elements for Parabolic Equations. In: *J. Comput. Math.* 25 (2007), Nr. 4, S. 385–407
- [3] ELLIOTT, C. M. ; RANNER, T.: Finite element analysis for a coupled bulk–surface partial differential equation. In: *IMA Journal of Numerical Analysis* (2012). <http://dx.doi.org/10.1093/imanum/drs022>. – DOI 10.1093/imanum/drs022
- [4] GORYACHEV, Andrew B. ; POKHILKO, Alexandra V.: Dynamics of Cdc42 network embodies a Turing-type mechanism of yeast cell polarity. In: *FEBS Lett* 582 (2008), Apr, Nr. 10, 1437–1443. <http://dx.doi.org/10.1016/j.febslet.2008.03.029>. – DOI 10.1016/j.febslet.2008.03.029
- [5] GRONWALL, T. H.: An inequality for the Bessel functions of the first kind with imaginary argument. In: *Ann. of Math. (2)* 33 (1932), Nr. 2, 275–278. <http://dx.doi.org/10.2307/1968329>. – DOI 10.2307/1968329. – ISSN 0003–486X
- [6] HELLANDER, Andreas ; HELLANDER, Stefan ; LTSTEDT, Per: Coupled mesoscopic and microscopic simulation of stochastic reaction-diffusion processes in mixed dimensions. In: *Multiscale Modeling & Simulation* 10 (2012), Nr. 2, S. 585–611
- [7] IFANTIS, E. K. ; SIAFARIKAS, P. D.: Inequalities involving Bessel and modified Bessel functions. In: *J. Math. Anal. Appl.* 147 (1990), Nr. 1, 214–227. [http://dx.doi.org/10.1016/0022-247X\(90\)90394-U](http://dx.doi.org/10.1016/0022-247X(90)90394-U). – DOI 10.1016/0022-247X(90)90394-U. – ISSN 0022–247X
- [8] JILKINE, Alexandra ; EDELSTEIN-KESHET, Leah: A comparison of mathematical models for polarization of single eukaryotic cells in response to guided cues. In: *PLoS Comput Biol* 7 (2011), Apr, Nr. 4, e1001121. <http://dx.doi.org/10.1371/journal.pcbi.1001121>. – DOI 10.1371/journal.pcbi.1001121
- [9] KELLER, Jürgen U.: An Outlook on Biothermodynamics. II. Adsorption of Proteins. In: *Journal of Non-Equilibrium Thermodynamics* 34 (2009), März, Nr. 1, 1–33. <http://dx.doi.org/10.1515/JNETDY.2009.001>. – ISSN 0340–0204
- [10] KHOLODENKO, B. N. ; HOEK, J. B. ; WESTERHOFF, H. V.: Why cytoplasmic signalling proteins should be recruited to cell membranes. In: *Trends Cell Biol* 10 (2000), May, Nr. 5, S. 173–178
- [11] KOCKELKOREN, J. ; LEVINE, H. ; RAPPEL, W.-J.: Computational approach for modeling intra- and extracellular dynamics. In: *Phys. Rev. E* 68 (2003), Sep, 037702. <http://dx.doi.org/10.1103/PhysRevE.68.037702>. – DOI 10.1103/PhysRevE.68.037702
- [12] KOKOLOGIANNAKI, C. G.: Bounds for functions involving ratios of modified Bessel functions. In: *J. Math. Anal. Appl.* 385 (2012), Nr. 2, 737–742. <http://dx.doi.org/10.1016/j.jmaa.2011.07.004>. – DOI 10.1016/j.jmaa.2011.07.004. – ISSN 0022–247X
- [13] LEVINE, H. ; RAPPEL, W.-J.: Membrane-bound Turing patterns. In: *Phys. Rev. E (3)* 72 (2005), Nr. 6, 061912, 5. <http://dx.doi.org/10.1103/PhysRevE.72.061912>. – DOI 10.1103/PhysRevE.72.061912. – ISSN 1539–3755
- [14] LI, X. ; LOWENGRUB, J. ; RÄTZ, A. ; VOIGT, A.: Solving PDEs in complex geometries: a diffuse domain approach. In: *Commun. Math. Sci.* 7 (2009), Nr. 1, S. 81–107
- [15] NOVAK, I. L. ; GAO, F. ; CHOI, Y.-S. ; RESASCO, D. ; SCHAFF, J. C. ; SLEPCHENKO, B. M.: Diffusion on a curved surface coupled to diffusion in the volume: application to cell biology. In: *J. Comput. Phys.* 226 (2007), Nr. 2, 1271–1290. <http://dx.doi.org/10.1016/j.jcp.2007.05.025>. – DOI 10.1016/j.jcp.2007.05.025. – ISSN 0021–9991
- [16] OLVER, F. W. J. (Hrsg.) ; LOZIER, D. W. (Hrsg.) ; BOISVERT, R. F. (Hrsg.) ; CLARK, C. W. (Hrsg.): *NIST Handbook of Mathematical Functions*. New York, NY : Cambridge University Press, 2010. – Print companion to [1]
- [17] RÄTZ, A. ; RÖGER, M.: Turing instabilities in a mathematical model for signaling networks. In: *J. Math. Biol.* 65 (2012), Nr. 6, S. 1215–1244
- [18] RÄTZ, A. ; VOIGT, A.: PDE’s on surfaces — a diffuse interface approach. In: *Comm. Math. Sci.* 4 (2006), Nr. 3, S. 575 – 590

- [19] RÄTZ, Andreas ; RÖGER, Matthias: Erratum to: Turing instabilities in a mathematical model for signaling networks. In: *J. Math. Biol.* 66 (2013), Nr. 1-2, 421–422. <http://dx.doi.org/10.1007/s00285-012-0630-x>. – DOI 10.1007/s00285-012-0630-x. – ISSN 0303-6812
- [20] TEIGEN, Knut E. ; LI, Xiangrong ; LOWENGRUB, John ; WANG, Fan ; VOIGT, Axel: A diffuse-interface approach for modeling transport, diffusion and adsorption/desorption of material quantities on a deformable interface. In: *Commun. Math. Sci.* 7 (2009), Nr. 4, S. 1009–1037
- [21] VEY, S. ; VOIGT, A.: AMDiS — Adaptive multidimensional simulations. In: *Comput. Visual. Sci.* 10 (2007), S. 57–67

ANDREAS RÄTZ, TECHNISCHE UNIVERSITÄT DORTMUND, FAKULTÄT FÜR MATHEMATIK, VOGELPOTHSWEG 87, D-44227 DORTMUND

*E-mail address:* `andreas.raetz@tu-dortmund.de`

MATTHIAS RÖGER, TECHNISCHE UNIVERSITÄT DORTMUND, FAKULTÄT FÜR MATHEMATIK, VOGELPOTHSWEG 87, D-44227 DORTMUND

*E-mail address:* `matthias.roeger@tu-dortmund.de`

## Preprints ab 2011/05

- 2013-07 **Andreas Rätz and Matthias Röger**  
Symmetry breaking in a bulk-surface reaction-diffusion model for signaling networks
- 2013-06 **Gilles Francfort and Ben Schweizer**  
A doubly non-linear system in small-strain visco-plasticity
- 2013-05 **Tomáš Dohnal**  
Traveling Solitary Waves in the Periodic Nonlinear Schrödinger Equation with Finite Band Potentials
- 2013-04 **Karl Friedrich Siburg, Pavel Stoimenov, and Gregor N.F. Weiß**  
Forecasting Portfolio-Value-at-Risk with Nonparametric Lower Tail Dependence Estimates
- 2013-03 **Martin Heida**  
On thermodynamics of fluid interfaces
- 2013-02 **Martin Heida**  
Existence of solutions for two types of generalized versions of the Cahn-Hilliard equation
- 2013-01 **T. Dohnal, A. Lamacz, B. Schweizer**  
Dispersive effective equations for waves in heterogeneous media on large time scales
- 2012-19 **Martin Heida**  
On gradient flows of nonconvex functionals in Hilbert spaces with Riemannian metric and application to Cahn-Hilliard equations
- 2012-18 **R.V. Kohn, J. Lu, B. Schweizer, and M.I. Weinstein**  
A variational perspective on cloaking by anomalous localized resonance
- 2012-17 **Margit Rösler and Michael Voit**  
Olshanski spherical functions for infinite dimensional motion groups of fixed rank
- 2012-16 **Selim Esedoğlu, Andreas Rätz, Matthias Röger**  
Colliding Interfaces in Old and New Diffuse-interface Approximations of Willmore-flow
- 2012-15 **Patrick Henning, Mario Ohlberger and Ben Schweizer**  
An adaptive multiscale finite element method
- 2012-14 **Andreas Knauf, Frank Schulz, Karl Friedrich Siburg**  
Positive topological entropy for multi-bump magnetic fields
- 2012-13 **Margit Rösler, Tom Koornwinder, and Michael Voit**  
Limit transition between hypergeometric functions of type BC and Type A
- 2012-12 **Alexander Schnurr**  
Generalization of the Blumenthal-Gettoor Index to the Class of Homogeneous Diffusions with Jumps and some Applications
- 2012-11 **Wilfried Hazod**  
Remarks on pseudo stable laws on contractible groups
- 2012-10 **Waldemar Grundmann**  
Limit theorems for radial random walks on Euclidean spaces of high dimensions



- 2012-09 **Martin Heida**  
A two-scale model of two-phase flow in porous media ranging from porespace to the macro scale
- 2012-08 **Martin Heida**  
On the derivation of thermodynamically consistent boundary conditions for the Cahn-Hilliard-Navier-Stokes system
- 2012-07 **Michael Voit**  
Uniform oscillatory behavior of spherical functions of  $GL_n/U_n$  at the identity and a central limit theorem
- 2012-06 **Agnes Lamacz and Ben Schweizer**  
Effective Maxwell equations in a geometry with flat rings of arbitrary shape
- 2012-05 **Frank Klinker and Günter Skoruppa**  
Ein optimiertes Glättungsverfahren motiviert durch eine technische Fragestellung
- 2012-04 **Patrick Henning, Mario Ohlberger, and Ben Schweizer**  
Homogenization of the degenerate two-phase flow equations
- 2012-03 **Andreas Rätz**  
A new diffuse-interface model for step flow in epitaxial growth
- 2012-02 **Andreas Rätz and Ben Schweizer**  
Hysteresis models and gravity fingering in porous media
- 2012-01 **Wilfried Hazod**  
Intrinsic topologies on H-contraction groups with applications to semistability
- 2011-14 **Guy Bouchitté and Ben Schweizer**  
Plasmonic waves allow perfect transmission through sub-wavelength metallic gratings
- 2011-13 **Waldemar Grundmann**  
Moment functions and Central Limit Theorem for Jacobi hypergroups on  $[0, \infty[$
- 2011-12 **J. Koch, A. Rätz, and B. Schweizer**  
Two-phase flow equations with a dynamic capillary pressure
- 2011-11 **Michael Voit**  
Central limit theorems for hyperbolic spaces and Jacobi processes on  $[0, \infty[$
- 2011-10 **Ben Schweizer**  
The Richards equation with hysteresis and degenerate capillary pressure
- 2011-09 **Andreas Rätz and Matthias Röger**  
Turing instabilities in a mathematical model for signaling networks
- 2011-08 **Matthias Röger and Reiner Schätzle**  
Control of the isoperimetric deficit by the Willmore deficit
- 2011-07 **Frank Klinker**  
Generalized duality for k-forms
- 2011-06 **Sebastian Aland, Andreas Rätz, Matthias Röger, and Axel Voigt**  
Buckling instability of viral capsides - a continuum approach
- 2011-05 **Wilfried Hazod**  
The concentration function problem for locally compact groups revisited: Non-dissipating space-time random walks,  $\tau$ -decomposable laws and their continuous time analogues